

# Numerical analysis of the rebellious voter model

Jan M. Swart\*

Karel Vrbenský \*

June 7, 2018

## Abstract

The rebellious voter model, introduced by Sturm and Swart (2008), is a variation of the standard, one-dimensional voter model, in which types that are locally in the minority have an advantage. It is related, both through duality and through the evolution of its interfaces, to a system of branching annihilating random walks that is believed to belong to the ‘parity-conservation’ universality class. This paper presents numerical data for the rebellious voter model and for a closely related one-sided version of the model. Both models appear to exhibit a phase transition between noncoexistence and coexistence as the advantage for minority types is increased. For the one-sided model (but not for the original, two-sided rebellious voter model), it appears that the critical point is exactly a half and two important functions of the process are given by simple, explicit formulas, a fact for which we have no explanation.

*MSC 2000.* Primary: 82C22; Secondary: 65C05, 82C26, 60K35

*Keywords.* Rebellious voter model, parity conservation, exactly solvable model, coexistence, interface tightness, cancellative systems, Markov chain Monte Carlo.

*Acknowledgements.* Work sponsored by GAČR grant 201/06/1323 and MŠMT ČR grant DAR 1M0572. We thank Ivan Dornic, as well as two referees, for many useful comments, especially on the physical side of the problem.

## Contents

|          |   |           |
|----------|---|-----------|
| <b>1</b> | <b>Introduction</b>                                     | <b>2</b>  |
| <b>2</b> | <b>Set-up and basic properties</b>                      | <b>3</b>  |
| 2.1      | Definition of the models . . . . .                      | 3         |
| 2.2      | Interface and dual models . . . . .                     | 5         |
| 2.3      | Coexistence, survival and interface tightness . . . . . | 6         |
| <b>3</b> | <b>Main results</b>                                     | <b>7</b>  |
| 3.1      | Methods . . . . .                                       | 7         |
| 3.2      | A first qualitative look . . . . .                      | 8         |
| 3.3      | The two-sided model . . . . .                           | 9         |
| 3.4      | The one-sided model . . . . .                           | 11        |
| 3.5      | Finite size effects . . . . .                           | 14        |
| <b>4</b> | <b>Other functions of the process</b>                   | <b>17</b> |
| 4.1      | Harmonic functions . . . . .                            | 17        |
| 4.2      | Frequencies for three and more particles . . . . .      | 20        |
| 4.3      | Edge speeds . . . . .                                   | 22        |
| <b>5</b> | <b>Conclusions</b>                                      | <b>23</b> |

---

\*swart@utia.cas.cz and vrbensky@utia.cas.cz, Institute of Information Theory and Automation of the ASCR (ÚTIA), Pod vodárenskou věží 4, 18208 Praha 8, Czech Republic. URL <http://staff.utia.cas.cz/swart/>

# 1 Introduction

The study of parity preserving branching-annihilating particle systems has a long history in the physics literature. Their main interest lies in the fact that they provide a rare example of systems that exhibit a phase transition of survival/extinction type (the physics literature usually speaks of a transition between an ‘active’ and an ‘absorbing’ phase) that does not belong to the directed percolation (DP) universality class.

Indeed, the phase transition of these models appears to belong to a different ‘parity conservation’ (PC) universality class, characterized by its own critical exponents. The first example of a phase transition belonging to this universality class was described in [GKT84]; this concerned a one-dimensional model for interfaces, motivated by solid state physics. Numerical simulations for parity preserving branching-annihilating particle systems on  $\mathbb{Z}^d$  in dimensions  $d = 1, 2, 3$  and also on Sierpinski gaskets can be found in [TT92]. Further simulations for a one-dimensional model were made in [Jen94]. This paper also contains the conjecture that the order parameter critical exponent  $\beta$  equals  $13/14$ ; in another paper the author has conjectured that  $\beta = 1$ . The latter value was also found in [IT98], while more recent literature seems to agree on a value of  $\beta \approx 0.92$  or slightly higher, see e.g. [Hin00, OS05]. Our present work is relevant to the question of determining the value of  $\beta$  since our proposed explicit formula for the survival probability  $\rho$  of the one-sided rebellious voter model, if it is correct, implies that  $\beta = 1$ .

Field-theoretic (renormalization group) work on the PC universality class was carried out in [CT98], who found two critical dimensions. The (usual) upper critical dimension is  $d_c = 2$ , above which one should find mean-field exponents. There is, however, a second critical dimension  $d'_c \approx 4/3$  such that only in dimensions below  $d'_c$  there is a nontrivial absorbing phase. From the field-theoretical perspective, the existence of a second critical dimension leads to considerable difficulties, to which the authors of [CCDDM05] reacted by considering non-perturbative techniques.

As usual, mathematical theory lags far behind theoretical physics and occupies itself with more basic and partially different questions. In particular, renormalization group techniques are generally nonrigorous and the existence of critical exponents or their universality below the upper critical dimension are from the mathematical perspective unproved conjectures. Nevertheless, in recent years, some rigorous mathematical work has been carried out on models (supposedly) belonging to the PC universality class. Sudbury [Sud90] studied a ‘double branching annihilation random walk’ (DBARW), which is a one-dimensional model for parity preserving branching-annihilating particles. The DBARW that can be exactly solved, in a certain sense, but unfortunately the model is in the absorbing phase for all nontrivial values of its parameter, hence there is no ‘true’ phase transition. (Nevertheless, its solution has been used in papers such as [CT98] to draw conclusions that presumably hold for the whole PC universality class.) No solvable models seem to be known so far that exhibit a true phase transition. (Below, we will present a possible candidate for such a model, the one-sided rebellious voter model.)

Strong impetus to the mathematical study of models from the PC universality class came from the paper of Neuhauser and Pacala [NP99], which proposes a variation on the  $d$ -dimensional range- $N$  voter model motivated by applications in population biology. Their model is governed by two parameters  $\alpha_0, \alpha_1$ . Here  $\alpha_i \leq 1$  models the *interspecific competition rate*, i.e., the death rate of organisms of type  $i$  due to competition with organisms of the other type, while the *intraspecific competition rate* is supposed to be one. In the symmetric

case  $\alpha_0 = \alpha_1 = \alpha$ , their model is dual to a system of parity preserving branching-annihilating random walks, with branching rate  $1 - \alpha$ . For  $d = 1, N = 1$ , up to a rescaling of time, this dual model is the DBARW; results for the latter imply that the model of Neuhauser and Pacala with  $d = 1, N = 1$  exhibits noncoexistence for all  $\alpha > 0$ . For  $N \geq 2$  and  $d = 1$ , their model is supposed to exhibit a nontrivial phase transition between coexistence and noncoexistence. For  $d = 2$ , their model is supposed to exhibit noncoexistence only for  $\alpha = 1$  while in dimensions  $d \geq 3$  noncoexistence holds for all  $\alpha$ , in line with the predictions made in [CT98].

Much of this lacks rigorous proof. First of all, it is not rigorously known that coexistence is a decreasing property in  $\alpha$ , or, in terms of the dual model, that increasing the branching rate leads to more particles in the system. Obvious as this may seem, finding a rigorous proof seems hard. Second, there exists no rigorous proof of noncoexistence (or equivalently, the existence of an absorbing phase for the dual model) except in the trivial cases  $\alpha = 1$  (pure voter) or  $d = 1, N = 1$  (related to DBARW). On the other hand, there exist a number of rigorous results proving coexistence (or equivalently, the existence of an active phase for the dual model). Neuhauser and Pacala proved that their model exhibits coexistence for  $\alpha$  sufficiently close to zero for all values of  $d$  and  $N$  except  $d = 1, N = 1$ . In [CP06], it has been proved that the model of Neuhauser and Pacala exhibits coexistence in dimensions  $d \geq 3$  for  $\alpha$  sufficiently close to *one* (the case of intermediate  $\alpha$  is still open due to the lack of a proof of monotonicity in  $\alpha$ ). The analogue result in  $d = 2$  is proved in [CMP09].

Some similar models were introduced in [BEM06], who studied parity preserving branching-annihilating random walks which allow for more particles at one site, and [SS08a], who introduced the rebellious voter model that will be studied in the present paper. A simple numerical simulation of that model, run for illustrative purposes, seemed to suggest that the critical point of this model is exactly a half, which motivated the present work. In fact, our results show that the critical value for this particular model is not  $\frac{1}{2}$ , but a closely related, one-sided version of the model seems to have its critical point exactly at  $\alpha = \frac{1}{2}$  and may in some sense be exactly solvable.

## 2 Set-up and basic properties

### 2.1 Definition of the models

Let

$$\{0, 1\}^{\mathbb{Z}} := \{x = (x(i))_{i \in \mathbb{Z}} : x(i) \in \{0, 1\} \forall i \in \mathbb{Z}\} \quad (2.1)$$

be the space whose elements  $x$  are infinite arrays of zeroes and ones, situated on the integer lattice  $\mathbb{Z}$ . We will be interested in Markov processes taking values in  $\{0, 1\}^{\mathbb{Z}}$ . We will mainly focus on the *rebellious voter model* introduced in [SS08a], and a variation on this model, which we call the *one-sided rebellious voter model*. For expository reasons, we will also shortly discuss two other models, the *disagreement* and *swapping voter models*.

In the one-sided rebellious voter model, initially, each site  $i \in \mathbb{Z}$  has a type  $x(i) \in \{0, 1\}$  assigned to it, and these types are updated according to the following stochastic dynamics. Independently for each site  $i \in \mathbb{Z}$ , one constructs times  $0 < \tau_1(i) < \tau_2(i) < \dots$  according to a Poisson process with rate 1, i.e.,  $\tau_1(i) - 0, \tau_2(i) - \tau_1(i), \tau_3(i) - \tau_2(i), \dots$  are i.i.d. exponentially distributed with mean 1. At each time  $t = \tau_k(i)$ , with  $k = 1, 2, \dots$ , the type of site  $i$  is updated according to the following rules. With probability  $\alpha$ , the site  $i$  looks at the site  $i - 1$  on its left, and if the type of site  $i - 1$  is different from the type of  $i$ , then site  $i$  changes its type. With the remaining probability  $1 - \alpha$ , the site  $i$  looks at the two sites  $i - 2$  and  $i - 1$  on its

left, and if the type of site  $i - 2$  is different from the type of  $i - 1$ , then site  $i$  changes its type. If we let  $X_t(i)$  denote the type of site  $i$  at time  $t$ , then  $(X_t)_{t \geq 0}$  is a continuous-time Markov process taking values in  $\{0, 1\}^{\mathbb{Z}}$ , which we call the *one-sided rebellious voter model*. Another way of describing its dynamics is to say that in this model, for any  $i \in \mathbb{Z}$ , the process  $X$  makes the transition

$$x \mapsto x^{\{i\}} \quad \text{with rate} \quad \alpha 1_{\{x(i-1) \neq x(i)\}} + (1 - \alpha) 1_{\{x(i-2) \neq x(i-1)\}}, \quad (2.2)$$

where  $1_A$  denotes the indicator function of an event  $A$  and for any  $x \in \{0, 1\}^{\mathbb{Z}}$  and  $\Delta \subset \mathbb{Z}$ , we let

$$x^\Delta(j) := \begin{cases} 1 - x(j) & \text{if } j \in \Delta, \\ x(j) & \text{if } j \notin \Delta \end{cases} \quad (2.3)$$

denote the configuration obtained from  $x$  by changing the types of all sites in  $\Delta$ .

The original *rebellious voter model* as introduced in [SS08a] is similar to the process described above, except that sites do not only look to the left, but also to the right when deciding whether to update their type. More precisely, in this case, at each time  $\tau_k(i)$  as defined above, the site  $i$  decides, with probability  $1/2$  each, to look either to the left or to the right. If the site looks to the left, then its type is updated as before. If the site  $i$  looks to the right, then with probability  $\alpha$ , it looks at the site  $i + 1$  on its right, and if the types of  $i$  and  $i + 1$  are different, then  $i$  changes its type. With the remaining probability  $1 - \alpha$ , the site  $i$  looks at the two sites  $i + 1$  and  $i + 2$  on its right, and if the types of  $i + 1$  and  $i + 2$  differ from each other, then  $i$  changes its type. Another way of describing these dynamics is to say that in this model, for any  $i \in \mathbb{Z}$ , the process makes the transition

$$x \mapsto x^{\{i\}} \quad \text{with rate} \quad \frac{1}{2} \alpha (1_{\{x(i-1) \neq x(i)\}} + 1_{\{x(i) \neq x(i+1)\}}) + \frac{1}{2} (1 - \alpha) (1_{\{x(i-2) \neq x(i-1)\}} + 1_{\{x(i+1) \neq x(i+2)\}}). \quad (2.4)$$

We note that our description of the rebellious voter model differs a factor  $1/2$  in the speed of time in comparison to the original definition in [SS08a].

A third and fourth model, that we also shortly discuss in this introduction, are the *disagreement* and *swapping voter models*. The disagreement voter model evolves as

$$x \mapsto x^{\{i\}} \quad \text{with rate} \quad \alpha (1_{\{x(i-1) \neq x(i)\}} + 1_{\{x(i) \neq x(i+1)\}}) + (1 - \alpha) 1_{\{x(i-1) \neq x(i+1)\}}, \quad (2.5)$$

while the swapping voter model evolves as

$$\begin{aligned} x \mapsto x^{\{i\}} & \quad \text{with rate} & \alpha (1_{\{x(i-1) \neq x(i)\}} + 1_{\{x(i) \neq x(i+1)\}}), \\ x \mapsto x^{\{i, i+1\}} & \quad \text{with rate} & (1 - \alpha) 1_{\{x(i) \neq x(i+1)\}}. \end{aligned} \quad (2.6)$$

In case of the rebellious voter model and its one-sided counterpart, the parameter  $0 \leq \alpha \leq 1$  can be interpreted as the (interspecific) *competition parameter*. For  $\alpha = 1$ , the model is a standard, one-dimensional voter model, as first introduced in [CS73, HL75]. For  $\alpha < 1$ , one can check that the dynamics give an advantage to types that are locally in the minority. As a consequence, at least on a heuristic level, decreasing  $\alpha$  should make it harder for any type to die out. The rebellious voter model has been introduced in [SS08a] in an attempt to model the distribution of two closely related species where competition between organisms belonging to different species is less strong than competition between organisms of the same species.

## 2.2 Interface and dual models

The models introduced so far are in two ways related to parity preserving branching annihilating particle systems. First, if  $X$  is any of the models defined in (2.2) and (2.4)–(2.6), then setting

$$Y_t(i) := 1_{\{X_t(i) \neq X_t(i+1)\}} \quad (t \geq 0, i \in \mathbb{Z}) \quad (2.7)$$

defines a Markov process taking values in  $\{0, 1\}^{\mathbb{Z}}$  that we call the *interface model* associated with  $X$ . (The sites  $i$  such that  $X_t(i) \neq X_t(i+1)$  are called interfaces, or also *kinks* or *domain walls*.) Indeed, in case of the one-sided rebellious voter model, it is not hard to see that  $Y$  jumps as

$$y \mapsto y^{\{i, i+1\}} \quad \text{with rate} \quad \alpha 1_{\{y(i)=1\}} + (1 - \alpha) 1_{\{y(i-1)=1\}}, \quad (2.8)$$

where we use notation defined in (2.3). For the two-sided process, the dynamics of  $Y$  are given by

$$y \mapsto y^{\{i, i+1\}} \quad \text{with rate} \quad \frac{1}{2} \alpha (1_{\{y(i)=1\}} + 1_{\{y(i+1)=1\}}) + \frac{1}{2} (1 - \alpha) (1_{\{y(i-1)=1\}} + 1_{\{y(i+2)=1\}}) \quad (2.9)$$

(see [SS08a, Section 1.2]), while for the disagreement voter model we get the ‘swapping annihilating random walk’ (SARW)

$$y \mapsto y^{\{i, i+1\}} \quad \text{with rate} \quad \alpha (1_{\{y(i)=1\}} + 1_{\{y(i+1)=1\}}) + (1 - \alpha) 1_{\{y(i) \neq y(i+1)\}}, \quad (2.10)$$

and for swapping voter model we get

$$\begin{aligned} y \mapsto y^{\{i, i+1\}} & \quad \text{with rate} \quad \alpha (1_{\{y(i)=1\}} + 1_{\{y(i+1)=1\}}) \\ y \mapsto y^{\{i-1, i+1\}} & \quad \text{with rate} \quad (1 - \alpha) 1_{\{y(i)=1\}}. \end{aligned} \quad (2.11)$$

Following [Sud90], we call this latter model the double branching annihilating random walk (DBARW); very similar models (usually in discrete time) have been called BARW2 or BAW in the physics literature (see, e.g., [TT92]).

In each of these interface models, since  $Y$  always flips the types of two sites at once, it is easy to see that  $Y$  *preserves parity*, i.e., if  $Y$  is started in an initial state  $Y_0$  which contains a finite, even (resp. odd) number of ones, then  $Y_t$  contains an even (resp. odd) number of ones for each  $t \geq 0$ . In particular, if  $Y$  is started with an odd number of ones, then the ones can never completely die out.

There is a second relation between our models and parity preserving branching-annihilating particle systems, namely, through duality. Recall that two Markov processes  $X$  and  $Y$  with state spaces  $S_X$  and  $S_Y$  are *dual* to each other if there exists a function  $\psi$  defined on  $S_X \times S_Y$ , called *duality function*, such that

$$\mathbb{E}^x[\psi(X_t, y)] = \mathbb{E}^y[\psi(x, Y_t)] \quad (t \geq 0), \quad (2.12)$$

where  $\mathbb{E}^x$  (resp.  $\mathbb{E}^y$ ) denotes expectation with respect to the law of the process  $X$  (resp.  $Y$ ) started in  $X_0 = x$  (resp.  $Y_0 = y$ ). A necessary and sufficient condition for (2.12) is that

$$G_X \psi(\cdot, y)(x) = G_Y \psi(x, \cdot)(y) \quad (x \in S_X, y \in S_Y), \quad (2.13)$$

where  $G_X$  (resp.  $G_Y$ ) denotes the generator of  $X$  (resp.  $Y$ ). In typical applications, one considers  $\psi$  such that the functions  $(\psi(\cdot, y))_{y \in S_Y}$  and  $(\psi(x, \cdot))_{x \in S_X}$  are distribution determining.

In this case, the transition probabilities of  $X$  and  $Y$  determine each other uniquely through (2.12).

In our case, each of the voter models  $X$  we have introduced is a cancellative spin system in the sense of [Gri79], hence it is known that for each of these models, there exists a Markov process  $Y$  which is also a cancellative spin system and which is dual to  $X$  with the duality function  $\psi(x, y) := (-1)^{|xy|}$ , where for any  $x, y, z \in \{0, 1\}^{\mathbb{Z}}$  we let  $xy(i) := x(i)y(i)$  denote the componentwise product of  $x$  and  $y$ , and we write  $|z| := \sum_i z(i)$ . In this case, (2.12) implies that

$$\mathbb{P}[|X_t Y_0| \text{ is odd}] = \mathbb{P}[|X_0 Y_t| \text{ is odd}] \quad (t \geq 0) \quad (2.14)$$

whenever  $X$  and  $Y$  are independent (with arbitrary initial laws), where in order for our expressions to be well-defined we must assume that either  $|X_0|$  or  $|Y_0|$  is finite.

A special property of the rebellious voter model (that motivated its introduction in [SS08a]) is that its interface model and dual model coincide, i.e., if  $X$  is the rebellious voter model, then (2.14) holds for the same  $Y$ , with dynamics described in (2.9), that also describes the interfaces of  $X$ . One way of checking this is to verify (2.13); an alternative proof, based on the graphical representation of cancellative spin systems, is described at [SS08a, formula (1.8)]. For the one-sided rebellious voter model, the dual and interface models do not coincide, but its dual is the mirror image of its interface model, i.e., the one-sided rebellious voter model satisfies (2.14) for a model  $Y$  whose dynamics are described by (compare (2.8))

$$y \mapsto y^{\{i-1, i\}} \quad \text{with rate} \quad \alpha 1_{\{y(i)=1\}} + (1 - \alpha) 1_{\{y(i+1)=1\}}. \quad (2.15)$$

It turns out that the dual (in the sense of cancellative spin systems) of the disagreement model is the DBARW (which is the interface model of the swapping voter model) while the dual of the swapping voter model is the SARW (which is the interface model of the disagreement voter model) (see [SS08a, Section 2.1]). Note that in the SARW there is no branching, which has far-reaching consequences for both the disagreement and swapping voter models.

### 2.3 Coexistence, survival and interface tightness

It is easy to see that the constant configurations  $\underline{0}$  and  $\underline{1}$  are traps for the various voter models we have introduced. By definition, we say that a Markov process taking values in  $\{0, 1\}^{\mathbb{Z}^d}$  exhibits *coexistence* if there exists an invariant law that is concentrated on configurations that are not identically zero or one. It is known that nearest-neighbor voter models on  $\mathbb{Z}^d$  exhibit coexistence if and only if  $d > 2$ ; in particular, for  $\alpha = 1$ , our models, being one-dimensional voter models, do not exhibit coexistence. On the other hand, our models exhibit coexistence for  $\alpha = 0$  since in this case one can check that product measure with intensity a half is an invariant law.

The question is whether there is a nontrivial phase transition between coexistence and noncoexistence. For the disagreement and swapping voter models it turns out that this is not the case. Indeed, it can be rigorously proved [Sud90, NP99, SS08a] that these models exhibit noncoexistence for all  $\alpha > 0$ . On the other hand, it appears that the rebellious voter model and its one-sided counterpart do exhibit a nontrivial phase transition between coexistence and noncoexistence at some  $0 < \alpha_c < 1$ .

We will mainly be interested in two functions of our processes. It is said that a voter model *survives* if there is a positive probability that the process started with a single one never gets trapped in  $\underline{0}$ . In view of this, for the (one- or two-sided) rebellious voter model

with competition parameter  $\alpha$ , we will be interested in the *survival probability*

$$\rho(\alpha) := \mathbb{P}^{\delta_0} [X_t \neq \underline{0} \ \forall t \geq 0], \quad (2.16)$$

where  $\mathbb{P}^{\delta_0}$  denotes the law of the process started in  $X_0 = \delta_0$ , with  $\delta_0(i) := 1_{\{i=0\}}$ . It seems plausible that for many models of the type we are considering, survival is equivalent to coexistence. Indeed, using the fact that its interface and dual models coincide, this can be rigorously proved for the rebellious voter model [SS08a, Lemma 2]; the same proof works for the one-sided process. One of the main aims of the present paper is to obtain good numerical data for the function  $\rho$ .

The function  $\rho$  quantifies, in a sense, how strongly the process exhibits coexistence (see also formulas (2.7) and (3.1) below). We need a similar formula to quantify noncoexistence. For any  $i \in \mathbb{Z}$ , let  $x_i^{\text{H}} \in \{0, 1\}^{\mathbb{Z}}$ , defined as

$$x_i^{\text{H}}(j) := \begin{cases} 0 & \text{if } j < i, \\ 1 & \text{if } i \leq j \end{cases} \quad (2.17)$$

denote a ‘Heaviside’ configuration of zeros and ones that are ‘completely separated’. Following [CD95], we say that a model  $X$  (with given parameter  $\alpha$ ) exhibits *interface tightness* if

$$\chi(\alpha) := \lim_{t \rightarrow \infty} \mathbb{P}^{x_0^{\text{H}}} [X_t = x_i^{\text{H}} \text{ for some } i \in \mathbb{Z}] > 0, \quad (2.18)$$

i.e., if the process started in a Heaviside configuration spends a positive fraction of its time in such configurations. It is intuitively plausible that interface tightness implies noncoexistence. It is rigorously known that the swapping voter model exhibits interface tightness for all  $\alpha > 0$  [SS08b].

The main aim of the present paper is to obtain good numerical data for the functions  $\rho$  and  $\chi$ , both for the rebellious voter model and for its one-sided analogue.

## 3 Main results

### 3.1 Methods

In our simulations, we start the interface process  $Y$  of either the rebellious voter model or its one-sided counterpart with an odd number of ones on an interval of  $N$  sites with periodic boundary conditions. Note that in this case, because the number of ones is odd and because of the periodic boundary conditions, we can no longer represent  $Y$  as in (2.7), but the dynamics in (2.8) and (2.9), as well as the duality relation (2.14), still make sense. Since we start with one particle, because of parity conservation, the system cannot die out. Letting  $Y_\infty$  denote the process in equilibrium, we assume that for large  $N$ , the following approximations are valid:

$$\begin{aligned} \text{(i)} \quad & \rho(\alpha) \approx 2\mathbb{P}[Y_\infty(0) = 1] = \frac{2}{N}\mathbb{E}[|Y_\infty|], \\ \text{(ii)} \quad & \chi(\alpha) \approx \mathbb{P}[|Y_\infty| = 1]. \end{aligned} \quad (3.1)$$

The arguments why formula (3.1) (ii) should hold are obvious from (2.7) and (2.18). The justification of formula (3.1) (i) is more subtle. Let  $Y^{1/2}$  denote the interface process of the rebellious voter model on  $\mathbb{Z}$ , started in an initial law such that the  $(Y_0(i))_{i \in \mathbb{Z}}$  are independent

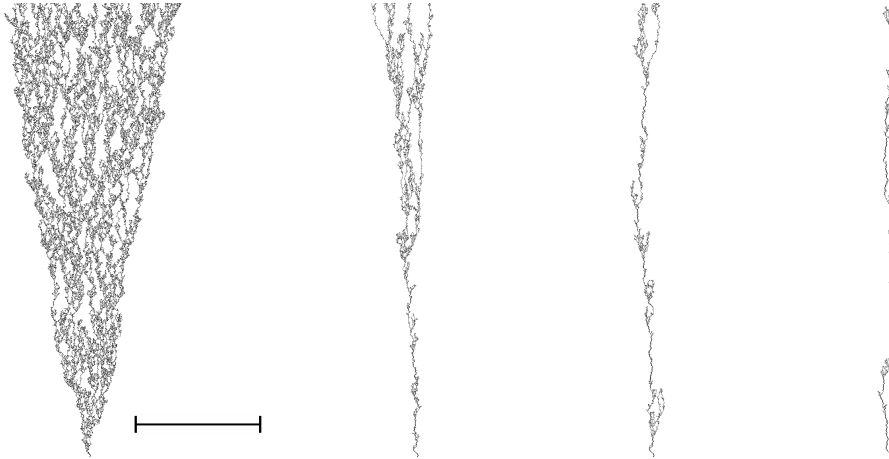


Figure 1: The interface model  $Y$  of the rebellious voter model for  $\alpha = 0.4$ ,  $\alpha = 0.5$ ,  $\alpha = 0.51$  and  $\alpha = 0.6$ , started with a single interface. Space is plotted horizontally and time vertically, with a black spot at a point  $(i, t)$  indicating that  $Y_t(i) = 1$ . Total time elapsed in each picture is 1800. The horizontal bar is 500 sites long.

with  $\mathbb{P}[Y_0(i) = 0] = \mathbb{P}[Y_0(i) = 1] = \frac{1}{2}$ , and let  $X$  be the rebellious voter model started in  $X_0 = \delta_0$ . Then by duality (2.14),

$$\mathbb{P}[Y_t^{1/2}(0) = 1] = \mathbb{P}[|Y_t^{1/2} X_0| \text{ is odd}] = \mathbb{P}[|Y_0^{1/2} X_t| \text{ is odd}] = \frac{1}{2} \mathbb{P}[X_t \neq \underline{0}], \quad (3.2)$$

where  $\underline{0}$  denotes the constant zero configuration. It is known that the law of  $Y_t^{1/2}$  converges as  $t \rightarrow \infty$  to an invariant law, which is in fact the unique spatially homogeneous, nontrivial invariant of the process [SS08a, formula (1.12) and Theorem 3 (b)]. Taking the limit  $t \rightarrow \infty$  in (3.2), we see that for this invariant law, formula (3.1) (i) holds with equality. Since it seems reasonable that the invariant laws of our finite systems approximate the invariant law of the infinite system, this justifies (3.1) (i). Similar arguments apply to the one-sided model.

### 3.2 A first qualitative look

Before we present our numerical data for the functions  $\rho$  and  $\chi$  from (3.1), we first take a look at the qualitative behavior of the interface model  $Y$  of the rebellious voter model and its one-sided analogue. In Figure 1, we have graphically plotted  $Y$  for the two-sided process, started with a single one, with time running upwards and a black spot at a point  $(i, t)$  indicating that  $Y_t(i) = 1$ . The figures shows the process for four values of  $\alpha$ , where  $\alpha_c \approx 0.51$  is the estimated critical value for this process (see Section 3.3 below).

The pictures show that for  $\alpha < \alpha_c$ , all ones are contained in an interval with edges that grow at an approximately linear speed, and that inside this interval, ones occur at some approximately constant equilibrium density. On the other hand, for  $\alpha > \alpha_c$ , the process spends a positive fraction of its time in states where there is just a single site in state one, which indicates that the rebellious voter model exhibits interface tightness (see (2.18)). What happens exactly at  $\alpha = \alpha_c$  is less clear from these pictures, but our numerical data, presented in Sections 3.3 and 4.3 below, suggest that at  $\alpha = \alpha_c$ , the edge speed is zero and the rebellious voter model exhibits neither coexistence nor interface tightness.



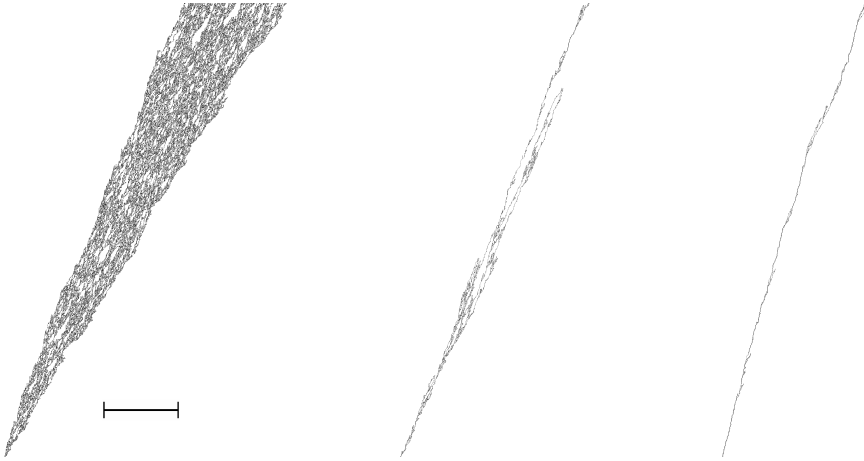


Figure 2: The interface model of the one-sided rebellious voter model for  $\alpha = 0.3$ ,  $\alpha = 0.5$  and  $\alpha = 0.6$ . Total time elapsed in each picture is 1800. The horizontal bar is 500 sites long.

The picture for the one-sided process is very similar, except that now, due to the nature of the process, the process as a whole tends to drift to the right at some approximately constant speed; see Figure 2.

### 3.3 The two-sided model

We simulated the interface model  $Y$  of the rebellious voter model on an interval of  $N$  sites with periodic boundary conditions by slowly increasing or decreasing  $\alpha$  from some initial value  $\alpha_b$  to some final value  $\alpha_e$  during a time interval of length  $T$ . We then divided our time interval into  $n$  equal pieces and plotted the average value of  $2|Y|/N$  (for the function  $\rho$ ) or the fraction of the time that  $|Y| = 1$  (for the function  $\chi$ ) against the average value of  $\alpha$ , for each of the  $n$  time intervals.

This method has both advantages and disadvantages. One of its main advantages is that it allows one to quickly obtain data for a very large number of values of the parameter, which is useful if one is interested in curve fitting or in estimating derivative functions such as in Figure 16. The method introduces obvious errors due to the nonzero speed of varying the parameter, but it is not difficult to get a rough idea of the size of these effects. In fact, one can get a good idea of the size of the errors just by looking at the curves (see Section 3.5 for a more detailed discussion). A disadvantage of the method is that the size of the errors varies a lot along the curves since relaxation times increase as one approaches the critical point. One can partially compensate for this by doing detailed simulations near the critical point. (A better approach, which we have not pursued, would be to vary  $\alpha$  at a suitable, precisely chosen nonconstant speed.)

The statistical errors in our data for the function  $\rho$  appear to be approximately normally distributed (with a variance that depends strongly on  $\alpha$ ), but those in the data for  $\chi$  have a skew distribution that is very far from a normal one (this is somewhat visible from Figure 7). This non-Gaussian behavior is not unexpected. Indeed, if we start the interface model  $Y$  in a state with  $|Y_0| = 3$  particles, then it is known that for the model with  $\alpha = 1$ ,

$$\mathbb{P}[\inf\{s \geq 0 : |Y_s| = 1\} \geq t] \sim t^{-3/2} \quad \text{as } t \rightarrow \infty. \quad (3.3)$$

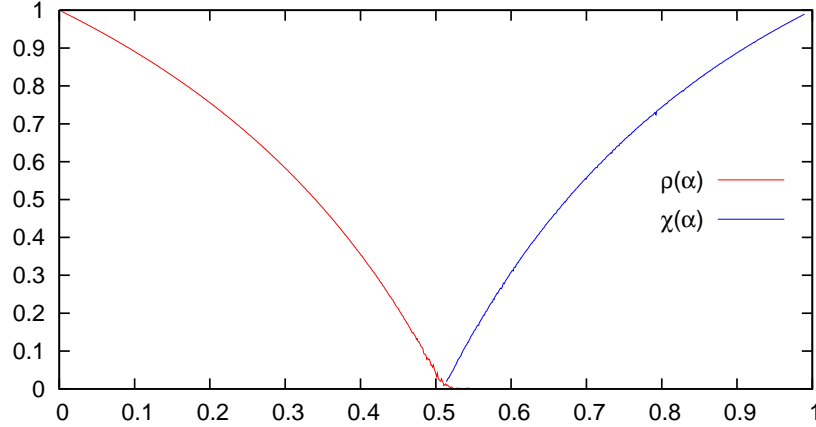


Figure 3: The functions  $\rho$  and  $\chi$  for the rebellious voter model. Data obtained with parameters as in (3.4).

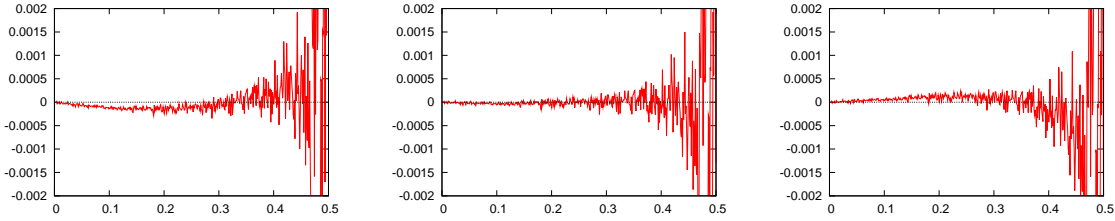


Figure 4: The function  $\rho(\alpha) - (1 - c_1\alpha)/(1 - c_2\alpha)$  for the values  $c_1 = 1.957$ ,  $c_2 = 0.973$  (left),  $c_1 = 1.958$ ,  $c_2 = 0.975$  (middle) and  $c_1 = 1.959$ ,  $c_2 = 0.977$  (right).

It seems natural to conjecture that this is also true for  $\alpha < 1$ , hence the process started with a single particle makes excursions into states with more than one particle that have a duration which has a finite first moment but infinite second moment.

In Figure 3 we have plotted approximations for the functions  $\rho$  and  $\chi$  obtained by our methods, using the parameters:

$$\begin{aligned} \text{for } \rho: & \quad N = 2^{15}, \quad n = 2^9, \quad T = 10^8, \quad \alpha_b = 0, \quad \alpha_e = 0.55, \\ \text{for } \chi: & \quad N = 2^{15}, \quad n = 2^9, \quad T = 10^{12}, \quad \alpha_b = 0.99, \quad \alpha_e = 0.49. \end{aligned} \quad (3.4)$$

The values  $\rho(0) = 1$  and  $\chi(1) = 1$  are expected on theoretical grounds. Indeed, it is easy to check that the rebellious voter model with  $\alpha = 0$  never dies out (recall (2.16)) while in the pure voter case  $\alpha = 1$ , the process started in a Heaviside state stays in such a state for all time (recall (2.18)).

The numerical data for  $\rho$  are well fitted by a linear fractional function of the form

$$\rho(\alpha) = \frac{1 - c_1\alpha}{1 - c_2\alpha} \quad \text{with} \quad c_1 = 1.958 \pm 0.001 \quad \text{and} \quad c_2 = 0.975 \pm 0.002, \quad (3.5)$$

(see Figure 4). Assuming this sort of function fitting is justified, we arrive at an estimate for the critical point of

$$\alpha_c = 0.5107 \pm 0.0003. \quad (3.6)$$

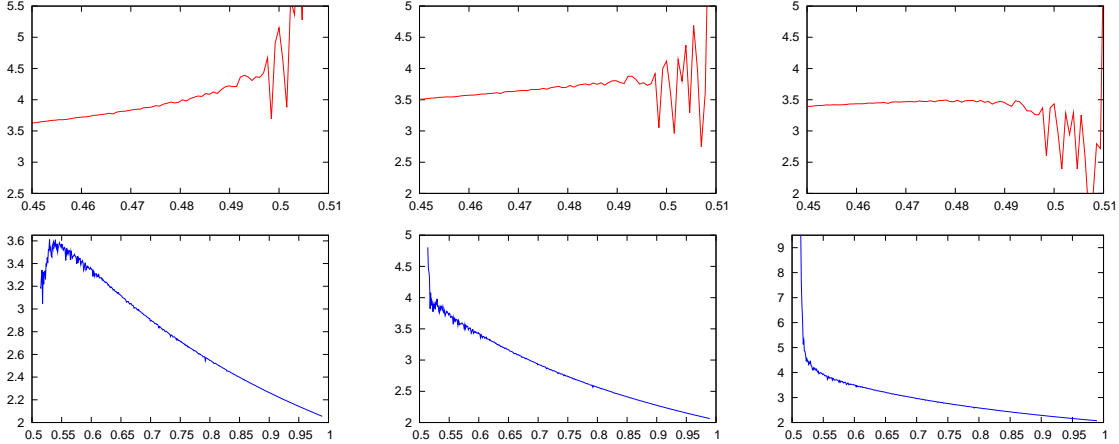


Figure 5: Estimation of the critical point of the rebellious voter model. Above: The function  $\rho(\alpha)/(\alpha - \alpha_0)$  for the values  $\alpha_0 = 0.508$  (left),  $\alpha_0 = 0.510$  (middle) and  $\alpha_0 = 0.512$  (right). Below: the function  $\chi(\alpha)/(\alpha - \alpha_0)$  for the values  $\alpha_0 = 0.508$  (left),  $\alpha_0 = 0.510$  (middle) and  $\alpha_0 = 0.512$  (right). Our simulations for  $\rho$  use the parameters  $N = 2^{15}$ ,  $n = 2^7$ ,  $T = 10^9$ ,  $\alpha_b = 0.55$ ,  $\alpha_e = 0.45$  and those for  $\chi$  use the parameters in (3.4).

This estimate is to be viewed with caution, since this is based on extrapolation of data for (approximately)  $0 \leq \alpha \leq 0.35$ , assuming that the linear fractional form (3.5) holds for all  $\alpha \leq \alpha_c$ . A more robust method (see Figure 5) based on our best data for the functions  $\rho$  and  $\chi$  near the critical point leads to the estimate:

$$\alpha_c = 0.510 \pm 0.002. \quad (3.7)$$

(See also Figure 9.) It seems that linear fractional functions do not fit the numerical data for  $\chi$  really well.

Our data strongly suggest that  $\rho(\alpha_c) = 0 = \chi(\alpha_c)$ , which implies that at criticality, the process exhibits neither coexistence nor interface stability. Summarizing, the picture that emerges from our numerical data is as follows:

There exists a critical value  $\alpha_c \approx 0.510$  such that the rebellious voter model exhibits coexistence if and only if  $\alpha < \alpha_c$  and interface tightness if and only if  $\alpha > \alpha_c$ . The function  $\rho$  from (2.16) has a finite negative slope and is concave on  $[0, \alpha_c]$ , and is approximately given by a linear fractional function of the form (3.5). The function  $\chi$  from (2.18) has a finite positive slope and is concave on  $[\alpha_c, 0]$ .

### 3.4 The one-sided model

We have run the same simulation as described in the previous section, with parameters as in (3.4), also for the one-sided rebellious voter model. The resulting approximations for the functions  $\rho$  and  $\chi$  are plotted in Figure 6.

At first sight, Figure 6 looks extremely similar to Figure 3. A closer inspection reveals, however, that the two plots are not identical. Indeed, it seems that for the one-sided model,

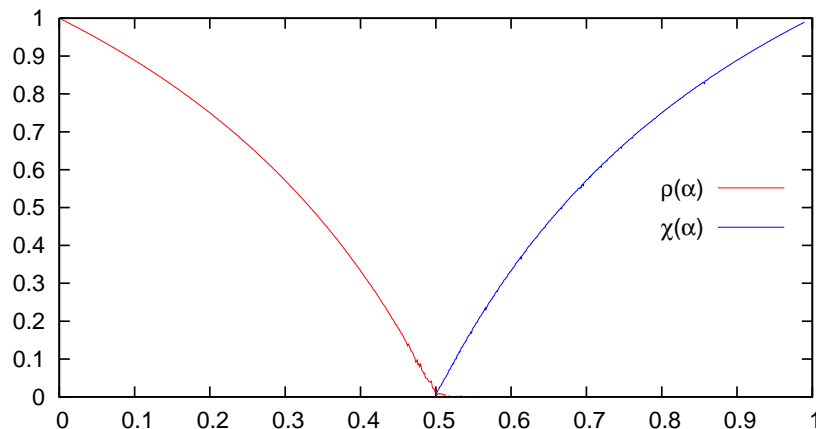


Figure 6: The functions  $\rho$  and  $\chi$  for the one-sided rebellious voter model. Data obtained with parameters as in (3.4).

the functions  $\rho$  and  $\chi$  are described by the explicit formulas:

$$\rho(\alpha) = 0 \vee \frac{1 - 2\alpha}{1 - \alpha} \quad \text{and} \quad \chi(\alpha) = 0 \vee \left(2 - \frac{1}{\alpha}\right). \quad (3.8)$$

In particular, one has the symmetry  $\rho(1 - \alpha) = \chi(\alpha)$  and the critical parameter seems to be given by

$$\alpha_c = 0.500 \pm 0.002 = \frac{1}{2} \quad (?) \quad (3.9)$$

In Figure 7, we have plotted the differences between the explicit functions in (3.8) and our data for  $\rho$  and  $\chi$ , respectively. The systematic deviations of  $\rho$  and  $\chi$  from the proposed formulas near the critical point probably stem from finite size effects (compare Figures 11 and 12 below). A more detailed comparison of  $\rho$  with its proposed explicit formula is shown in Figure 8. Because of the small difference between the left and right edge speed near the critical point (see Section 4.3), these detailed simulations are sensitive to the direction in which  $\alpha$  is varied (compare Figure 14 and the discussion in Section 3.5). In particular, the systematic deviation between our proposed explicit formula and the curve produced by lowering  $\alpha$  in the left plot of Figure 8 seems to stem from such effects. This systematic deviation almost disappears after giving the system more time to relax (see the right plot of Figure 8).

We guessed our formula for  $\rho$  after estimating the first few derivatives at  $\alpha = 0$  and the formula for  $\chi$  by analogy with  $\rho$ . We do not know of any theoretical reason to expect these formulas. A detailed comparison of the two-sided and one-sided model near the critical point is shown in Figure 9.

Our proposed explicit formula for  $\rho$ , if it is correct, implies that the order parameter critical exponent  $\beta$  for our model is one. Since this is different from the recently published values  $\beta = 0.92(2)$  [Hin00] and  $\beta = 0.95(1)$  [OM06] for the PC universality class, we have used our data to obtain a direct estimate for the value of  $\beta$ . A plot of  $\log(\rho)$  as a function of  $\log(\alpha_c - \alpha)$  yields an approximate linear graph as  $\alpha$  approximates  $\alpha_c$  from below, the slope of which should be  $\beta$ . To estimate this slope, in Figure 10 we have plotted  $\log(\rho) - \beta \log(\alpha_c - \alpha)$  as a function of  $-\log(\alpha_c - \alpha)$ , both for the two-sided and one-sided model, for different values of  $\beta$ . These plots are suggestive of a value of  $\beta$  that is perhaps closer to 0.92 than to 1, but

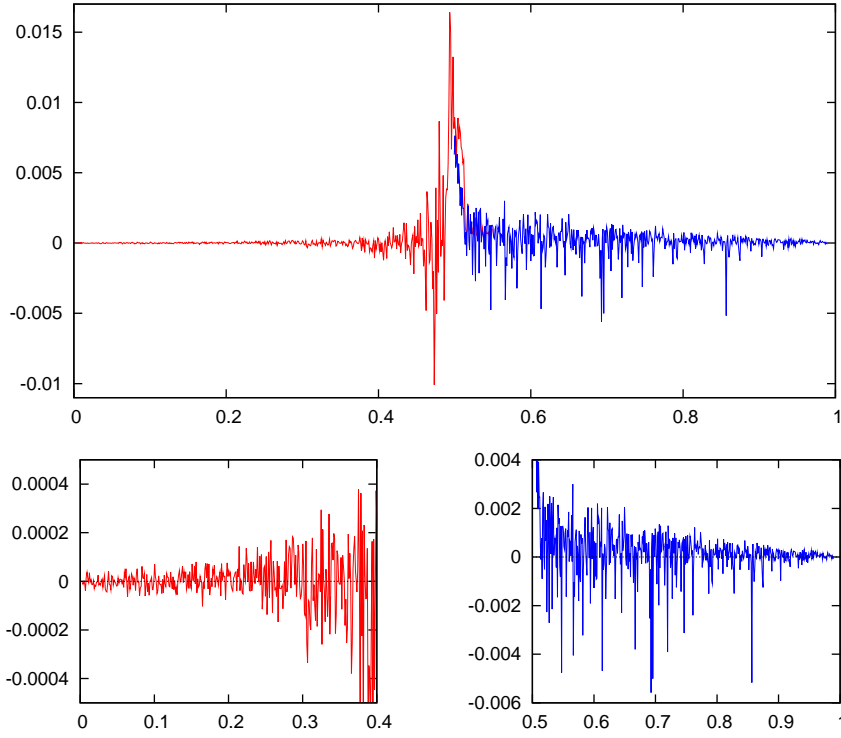


Figure 7: Difference between the explicit formulas in (3.8) and the functions  $\rho$  and  $\chi$  for the one-sided rebellious voter model, with detail of the left and right side of the picture.

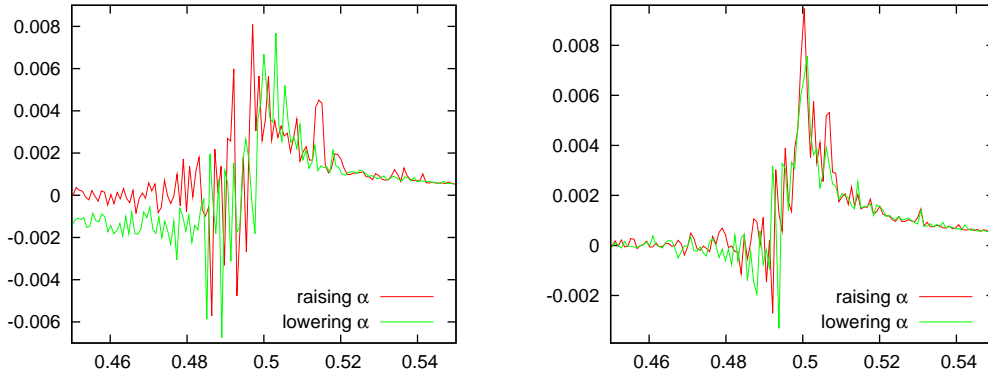


Figure 8: Plots of  $\rho(\alpha) - \max\{0, (1 - 2\alpha)/(1 - \alpha)\}$  for the one-sided rebellious voter model near the critical point. All plots use the parameters  $N = 2^{15}$ ,  $n = 2^7$ . On the left:  $T = 10^9$  and  $\alpha_b = 0.445$ ,  $\alpha_e = 0.55$  resp.  $\alpha_b = 0.55$  and  $\alpha_e = 0.45$ . On the right:  $T = 4 \cdot 10^9$  and  $\alpha_b = 0.445$ ,  $\alpha_e = 0.55$  resp.  $\alpha_b = 0.55$  and  $\alpha_e = 0.445$ .

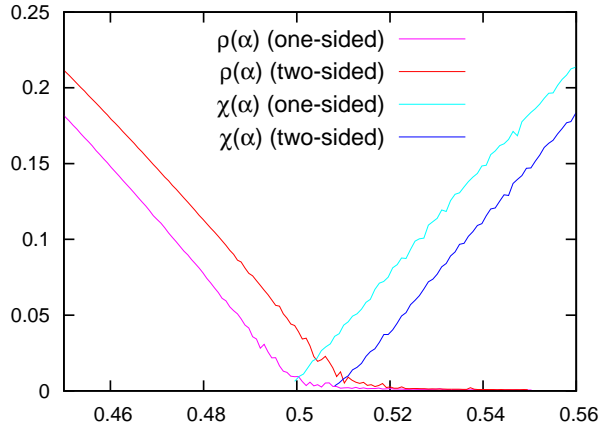


Figure 9: A detailed simulation near the critical point of the functions  $\rho$  and  $\chi$  for the two-sided process and the one-sided process. On the left: our simulations for  $\rho$  use the parameters  $N = 2^{15}$ ,  $n = 2^7$ ,  $T = 4 \cdot 10^9$ ,  $\alpha_b = 0.445$ ,  $\alpha_e = 0.55$ . Our plots for  $\chi$  show detail of a simulation with the parameters  $N = 2^{15}$ ,  $n = 2^9$ ,  $T = 10^{12}$ ,  $\alpha_b = 0.99$ ,  $\alpha_e = 0.5$ .

this is probably due to the fact that our simulations are not precise enough to get sufficiently close to the critical point. In fact, our data become unreliable at  $\alpha_c - \alpha \leq 0.004$ , which corresponds to the point  $-\log(0.004) \approx 5.5$  in Figure 10. Note that in Figure 8, for the one-sided model, the same data were shown to be consistent with our proposed explicit formula for  $\rho$  in (3.8), which, if true, implies that  $\beta = 1$ . We conclude that our data are not good enough to convincingly distinguish between  $\beta = 0.92$  and  $\beta = 1$ .

### 3.5 Finite size effects

To gain more insight into how close our numerical data are to the real functions  $\rho$  and  $\chi$ , we tested the effect of varying the system size  $N$ . In Figure 11 we have plotted our approximation (see (3.1)) of the function  $\rho$  for different values of the system size  $N$ . The pictures for the two-sided and one-sided process are extremely similar, except for a shift of the critical point. In view of Figure 11, it seems that we can rule out the possibility that the observed differences between the two-sided and one-sided process are due to finite space effects (and a hypothetical slower convergence for the two-sided model).

Note that in Figure 11, our approximations to  $\rho$  near the critical point become more rough as the system size is increased. This can be understood due to two effects. On the one hand, near criticality, the random variable  $|Y_\infty|$  assumes the values  $1, 3, 5, 7, \dots$  with approximately equal probabilities (see Section 4.2), which means that the number of ones in the system fluctuates from being close to one to a positive fraction of all sites in the lattice. As the system size gets large, this means huge fluctuations, which are moreover slow since at criticality, the edge speed is zero.

In Figure 12, we have plotted our approximations for the function  $\chi$  for various values of  $N$ . To counteract the ‘roughening’ effect we have just described, in these simulations, we have increased the total time  $T$  together with the system size  $N$ . Again, the pictures for the two-sided and one-sided process are similar except for a small shift in the critical point.

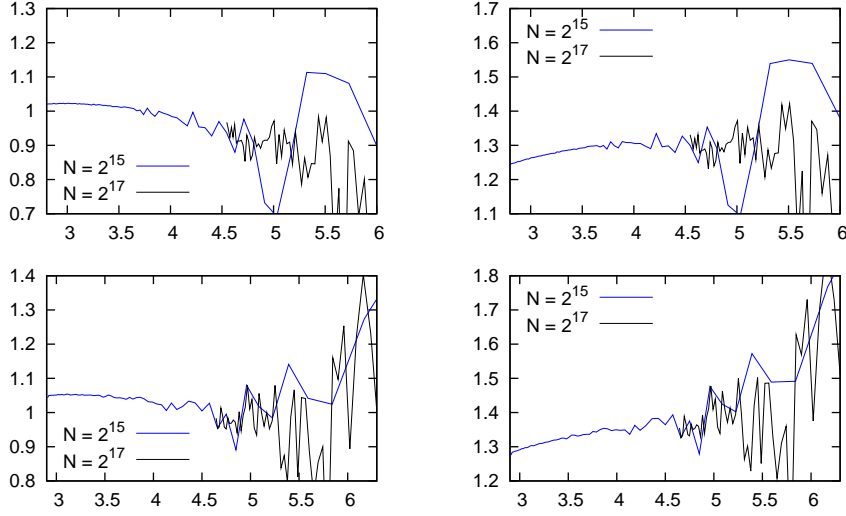


Figure 10: Estimation of the order parameter critical exponent  $\beta$ . Plots of  $\log(\rho) - \beta \log(\alpha_c - \alpha)$  as a function of  $-\log(\alpha_c - \alpha)$ . For the right choice of  $\beta$ , the asymptotic slope of these functions should be zero as the parameter on the horizontal axis tends to infinity. Above: plots for the two-sided model with  $\beta = 0.92$  (left) and  $\beta = 1$  (right), based on the estimate  $\alpha_c = 0.51$ . Below: the same for the one-sided model, based on the estimate  $\alpha_c = 0.5$ . Each figure combines two plots, one based on simulations with the parameters  $N = 2^{15}$ ,  $n = 2^7$ ,  $T = 4 \cdot 10^9$ ,  $\alpha_b = 0.445$ ,  $\alpha_e = 0.55$ , the other instead using  $N = 2^{17}$  and a smaller range of alpha ( $\alpha_b = 0.5$ ,  $\alpha_e = 0.52$  for the two-sided model and  $\alpha_b = 0.49$ ,  $\alpha_e = 0.51$  for the one-sided model).

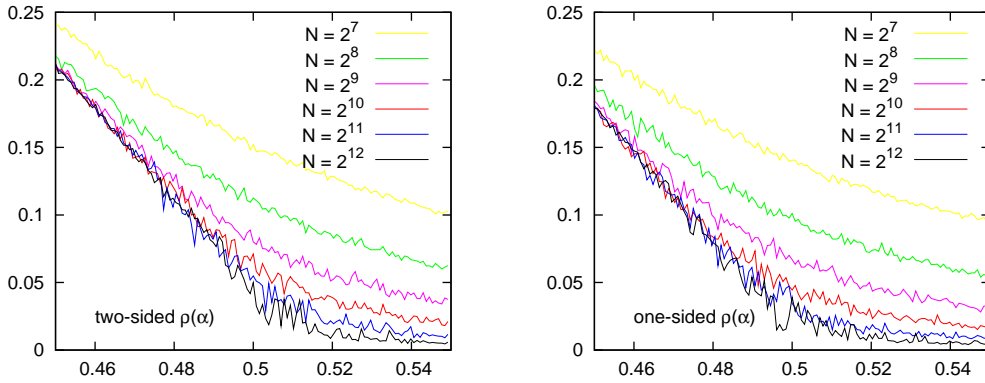


Figure 11: Effect of the system size on our approximation of the function  $\rho$  from (3.1). Plotted are our approximations for  $\rho$  using the parameters  $n = 2^7$ ,  $T = 10^8$ ,  $\alpha_b = 0.55$ ,  $\alpha_e = 0.45$ , and the system sizes  $N = 2^7, 2^8, 2^9, 2^{10}, 2^{11}, 2^{12}$ , respectively. On the left: the two-sided model. On the right: the one-sided model.

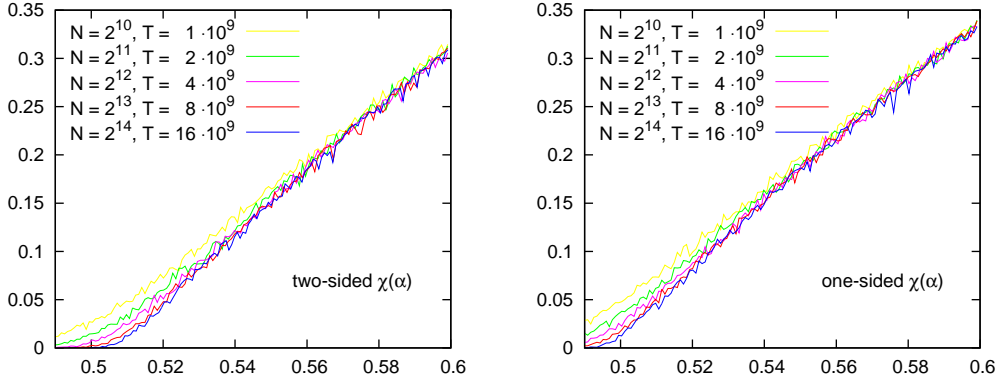


Figure 12: Effect of the system size on our approximation of the function  $\chi$  from (3.1). Plotted are our approximations for  $\chi$  using the parameters  $n = 2^7$ ,  $\alpha_b = 0.6$ ,  $\alpha_e = 0.49-0.5$ , and the system sizes  $N = 2^{10}, 2^{11}, 2^{12}, 2^{13}, 2^{14}$  and times  $T = 10^9, 2 \cdot 10^9, 4 \cdot 10^9, 8 \cdot 10^9, 16 \cdot 10^9$ , respectively. On the left: the two-sided model. On the right: the one-sided model.

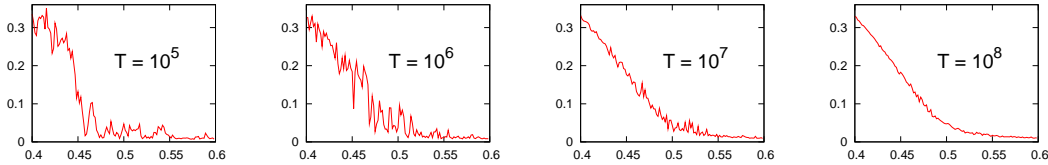


Figure 13: Effect of the duration of our simulations on our approximation of the function  $\rho$  from (3.1) for the one-sided model. Plotted are our approximations for  $\rho$  using the parameters  $N = 2^{10}$ ,  $n = 2^7$ ,  $\alpha_b = 0.6$ ,  $\alpha_e = 0.4$ , and the total elapsed times  $T = 10^5, 10^6, 10^7, 10^8$ , respectively.

We have also run simulations for different values of the total elapsed time, to investigate the effect of this parameter on the quality of our data. Since short times mean the system does not have enough time for time averages to reach their equilibrium values, the main effect of increasing  $T$  is to smoothen our approximated functions. For the function  $\rho$ , this effect is demonstrated in Figure 13. A second effect of choosing a too short time  $T$  is that the numerical functions ‘lag behind’ in that they show values belonging to an  $\alpha$  that lies somewhat in the past. This effect is demonstrated in Figure 14. In this case, our approximations near the critical point depend on the direction in which we vary  $\alpha$ : the graph produced by increasing  $\alpha$  ‘overshoots’ the critical point while the graph produced by lowering  $\alpha$  picks up too late. Also note the ‘hook’ at the beginning of the graph started with  $\alpha$  below the critical point, which is due to the fact that we start with a single one and the finite edge speed needs several time steps to fill out all space. This sort of effects only occur when  $T$  is small relative to  $N$ ; in all of our simulations (except those in Figure 14) we have done our best to choose our parameters such that these effects in minimal. In case of doubt, we have run the same simulation in both directions for comparison (see Figure 8). In some plots, we have removed a small ‘hook’ at the beginning.



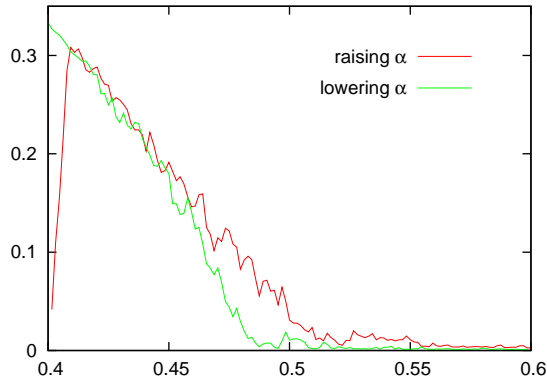


Figure 14: Effects of choosing the time too small compared to the system size, in simulations of  $\rho$  for the one-sided model. The two curves were produced by raising resp. lowering  $\alpha$  between the values  $\alpha_b$  resp.  $\alpha_e = 0.4$  and  $\alpha_e$  resp.  $\alpha_b = 0.6$ . The other simulation parameters were  $n = 2^7$ ,  $N = 2^{13}$ , and  $T = 10^6$ .

## 4 Other functions of the process

### 4.1 Harmonic functions

We have obtained numerical data for a number of other functions of our processes. We have mainly concentrated on the one-sided model, in view of the apparent explicit formulas for the functions  $\rho$  and  $\chi$  in this case. We have not been able, however, to find explicit formulas for any other functions than these two. Nevertheless, our additional functions show some interesting phenomena, which we discuss here. In the present section, we discuss a harmonic function for the (one-sided) rebellious voter model. In the next two sections, we look at the equilibrium probabilities of seeing 3, 5, 7, ... ones in the interface model, and edge speeds, respectively.

Recall that if  $X$  is a Markov process with state space  $S_X$ , then a function  $f : S_X \rightarrow \mathbb{R}$  is called a *harmonic function* for  $X$  if, for any initial state, the process  $(f(X_t))_{t \geq 0}$  is a martingale. At least for finite state spaces, this is equivalent to the statement that  $G_X f = 0$ , where  $G_X$  denotes the generator of  $X$ . In general, a duality between Markov processes translates the invariant laws of one process into harmonic functions of the other process. More precisely, if  $X$  and  $Y$  are dual Markov process, with duality function  $\psi$ , and  $\mu$  is an invariant measure for  $Y$ , then using (2.14) it is easy to see that setting

$$f(x) := \int_{S_Y} \psi(x, y) \mu(dy) \quad (x \in S_X) \quad (4.1)$$

defines a harmonic function  $f$  for  $X$ . Note that multiplying  $f$  with a constant will not change the fact that it is harmonic.

To apply this to the one-sided rebellious voter model, we first need to introduce some notation. In this section, we let  $X_t$  denote the rebellious voter model,  $\vec{X}_t$  the one-sided rebellious voter model, and  $\overleftarrow{X}_t$  the mirror image of the latter, i.e., the model that jumps as

$$x \mapsto x^{\{i\}} \quad \text{with rate} \quad \alpha 1_{\{x(i) \neq x(i+1)\}} + (1 - \alpha) 1_{\{x(i+1) \neq x(i+2)\}}. \quad (4.2)$$

We let  $\vec{Y}_t$  and  $\overleftarrow{Y}_t$  denote the interface models of  $\vec{X}_t$  and  $\overleftarrow{X}_t$ , respectively, i.e.,  $\vec{Y}_t$  is the process with dynamics described in (2.8) and  $\overleftarrow{Y}_t$  is the process in (2.15). Then  $\vec{Y}_t$  is dual to  $\vec{X}_t$  and  $\overleftarrow{Y}_t$  is dual to  $\overleftarrow{X}_t$ , in the sense of (2.14).

We consider  $\overleftarrow{Y}_t$  on an interval of  $N$  sites with periodic boundary conditions, started with an odd number of ones, and let  $\overleftarrow{Y}_\infty$  denote the process in equilibrium. For each  $x \in \{0, 1\}^N$ , we define

$$\vec{f}_{x,N}(\alpha) := \frac{\mathbb{P}[|x\overleftarrow{Y}_\infty| \text{ is odd}]}{\mathbb{P}[\overleftarrow{Y}_\infty(0) = 1]}. \quad (4.3)$$

By our previous remarks,  $\vec{f}_{x,N}(\alpha)$ , as a function of  $x$  for fixed  $\alpha$ , is a harmonic function for the one-sided rebellious voter model  $\vec{X}_t$ , on an interval of  $N$  sites with periodic boundary conditions. We will be interested in the limit of  $\vec{f}_{x,N}(\alpha)$  as  $N \rightarrow \infty$ , when  $x$  remains finite and fixed. In view of this, we only write down only the part of  $x$  that is nonzero. For example, we write  $\vec{f}_{1101,N}(\alpha)$  to denote the function  $\vec{f}_{x,N}(\alpha)$  where  $x$  is any element of  $\{0, 1\}^N$  such that  $(x(i), x(i+1), x(i+2), x(i+3)) = (1, 1, 0, 1)$  for some  $i \in \{0, \dots, N-1\}$  and  $x(j) = 0$  for all  $j \neq i, i+1, i+2, i+3$ . Note that since the law of  $\overleftarrow{Y}_\infty$  is translation invariant (modulo  $N$ ), this definition does not depend on the value of  $i$ .

Our simulations suggest that the functions  $\vec{f}_{x,N}(\alpha)$  converge as  $N \rightarrow \infty$  to a nontrivial limit function  $\vec{f}_x(\alpha)$ , which, as a function of  $x$  for fixed  $\alpha$ , is a harmonic function for the one-sided rebellious voter model  $\vec{X}_t$  on  $\mathbb{Z}$ , started with finitely many ones. If  $\alpha < \alpha_c$ , then on theoretical grounds one may expect that

$$\vec{f}_x(\alpha) = \frac{\vec{\rho}_x(\alpha)}{\vec{\rho}_1(\alpha)}, \quad \text{where} \quad \vec{\rho}_x(\alpha) := \mathbb{P}^x[\vec{X}_t \neq \underline{0} \forall t \geq 0] \quad (4.4)$$

denotes the probability that the one-sided rebellious voter model  $\vec{X}_t$  started in the initial state  $x$  survives. For  $\alpha > \alpha_c$ , in the regime where interface tightness holds, we can relate  $\vec{f}_x(\alpha)$  to the invariant law of the process  $\overleftarrow{Y}_t$ , started with a single one and viewed from its left-most one (see formula (4.19) below). Since we expect  $\vec{f}_x(\alpha)$  to be harmonic we expect that  $\vec{G}\vec{f}_x(\alpha) = 0$ , where  $\vec{G}$  is the generator of the one-sided rebellious voter model, which is given by

$$\vec{G}f_x = \sum_i (\alpha 1_{\{x(i-1) \neq x(i)\}} + (1-\alpha) 1_{\{x(i-2) \neq x(i-1)\}}) (f_{x^{(i)}} - f_x). \quad (4.5)$$

In particular, the facts that  $\vec{G}\vec{f}_1(\alpha) = 0$  and  $\vec{G}\vec{f}_{11}(\alpha) = 0$  lead to the relations

$$\begin{aligned} \alpha(\vec{f}_\emptyset(\alpha) - \vec{f}_1(\alpha)) + (\vec{f}_{11}(\alpha) - \vec{f}_1(\alpha)) + (1-\alpha)(\vec{f}_{101}(\alpha) - \vec{f}_1(\alpha)) &= 0, \\ \alpha(\vec{f}_{111}(\alpha) - \vec{f}_{11}(\alpha)) + (\vec{f}_1(\alpha) - \vec{f}_{11}(\alpha)) + (1-\alpha)(\vec{f}_{1101}(\alpha) - \vec{f}_{11}(\alpha)) &= 0, \end{aligned} \quad (4.6)$$

where  $\vec{f}_\emptyset(\alpha) = 0$  and  $\vec{f}_1(\alpha) = 1$ . An inspection of our numerical data shows that these equations are satisfied within the precision of our simulations.

Our numerical data for the functions  $\vec{f}_x(\alpha)$ , for some simple choices of the pattern  $x$ , are shown in Figure 15. Note that  $\vec{f}_1(x)$  (not shown in the figure) is by definition identically one, because of the normalization chosen in (4.3). A surprising fact is that the functions  $\vec{f}_x(\alpha)$  and their derivatives (shown in Figure 16) appear to continue smoothly across the critical point. Note that the normalization in (4.3) is crucial here, since above  $\alpha_c$ , both the numerator and the denominator tend to zero as  $N \rightarrow \infty$ . For  $\alpha = 1$  one has  $\vec{f}_x(\alpha) = |x|$ , which is a

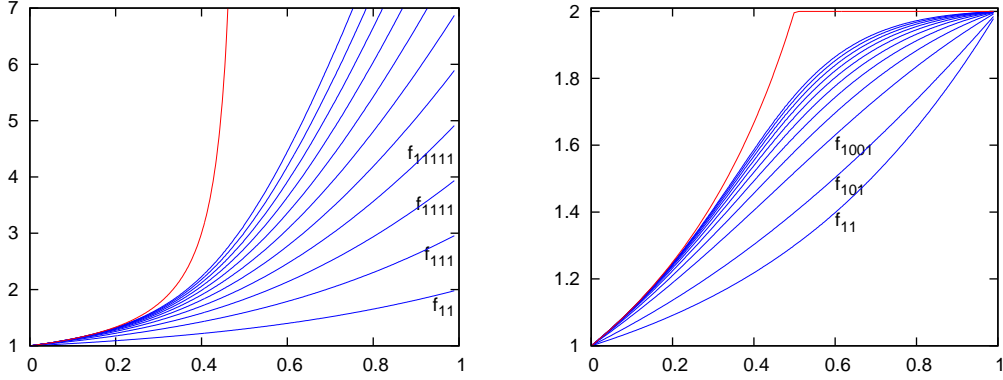


Figure 15: The functions  $\vec{f}_{11}, \vec{f}_{111}, \vec{f}_{1111}, \dots$  (left) and  $\vec{f}_{11}, \vec{f}_{101}, \vec{f}_{1001}, \dots$  (right). The functions in the left figure increase to the limit  $1/\rho(\alpha)$  while the functions in the right figure increase to  $2 - \rho(\alpha)$ . Both limits (theoretical curves) are plotted together with the data. The functions  $\vec{f}_{11}, \vec{f}_{111}, \vec{f}_{101}$  are based on data obtained with the parameters  $N = 2^{11}, n = 2^8, T = 10^8, \alpha_b = 0, \alpha_e = 0.5$  (left half of the pictures) and  $N = 2^{15}, n = 2^8, T = 10^9, \alpha_b = 0.99, \alpha_e = 0.51$  (right half of the pictures). The other functions are a combination of simulations using the parameters  $N = 2^{11}, n = 2^8, T = 10^8, \alpha_b = 0, \alpha_e = 0.5$  and  $N = 2^{15}, n = 2^8, T = 10^{10}, \alpha_b = 0.99, \alpha_e = 0.51$ .

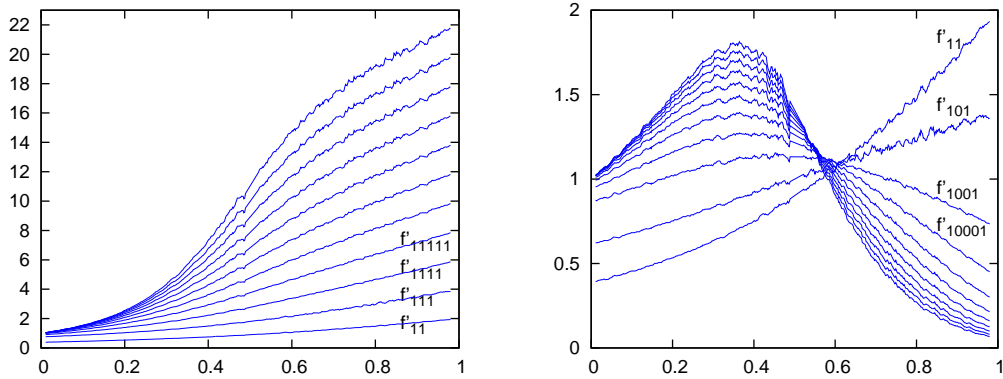


Figure 16: Derivatives of the functions from Figure 15. On the left  $\frac{\partial}{\partial \alpha} \vec{f}_{11}(\alpha), \frac{\partial}{\partial \alpha} \vec{f}_{111}(\alpha), \dots$ . On the right  $\frac{\partial}{\partial \alpha} \vec{f}_{11}(\alpha), \frac{\partial}{\partial \alpha} \vec{f}_{101}(\alpha), \frac{\partial}{\partial \alpha} \vec{f}_{1001}(\alpha), \dots$ . Figure based on the same data as Figure 15. The derivatives are estimated with a quadratic Savitzky-Golay filter using 11 data points.

well-known harmonic function for the pure voter model. For  $\alpha = 0$ , one has  $\vec{f}_x(\alpha) = 1$  for all nonzero  $x$ , reflecting the fact that the process with  $\alpha = 0$  never dies out.

A few regularities may be observed from Figures 15 and 16. Let

$$x_n := \underbrace{111111111}_{n \text{ ones}} \quad \text{and} \quad x'_n := \underbrace{10000001}_{n-2 \text{ zeros}}. \quad (4.7)$$

One expects that for  $\alpha < \alpha_c$ ,

$$\lim_{n \rightarrow \infty} \vec{\rho}_{x_n}(\alpha) = 1 \quad \text{and} \quad \lim_{n \rightarrow \infty} \vec{\rho}_{x'_n}(\alpha) = 1 - (1 - \vec{\rho}_1(\alpha))^2. \quad (4.8)$$

Hence, in view of (4.4), one expects that

$$\lim_{n \rightarrow \infty} \vec{f}_{x_n}(\alpha) = \vec{\rho}_1(\alpha)^{-1} \quad \text{and} \quad \lim_{n \rightarrow \infty} \vec{f}_{x'_n}(\alpha) = 2 - \vec{\rho}_1(\alpha), \quad (4.9)$$

which is indeed what we observe.

From Figure 16 we moreover observe that

$$\frac{\partial}{\partial \alpha} \vec{f}_{x_n}(\alpha) \Big|_{\alpha=1} = 2(n-1) \quad (n \geq 2). \quad (4.10)$$

This can be explained on theoretical grounds. Indeed, if we write  $\vec{G} = \alpha \vec{G}_{\text{vot}} + (1-\alpha) \vec{G}_{\text{reb}}$ , where  $\vec{G}_{\text{vot}}$  and  $\vec{G}_{\text{reb}}$  are the (one-sided) voter and rebellious parts of the generator, then a simple calculation shows that

$$\vec{G}_{\text{vot}} \frac{\partial}{\partial \alpha} \vec{f}_x(\alpha) \Big|_{\alpha=1} = \vec{G}_{\text{reb}} \vec{f}_x(1). \quad (4.11)$$

Setting  $g_x := \frac{\partial}{\partial \alpha} \vec{f}_x(\alpha) \Big|_{\alpha=1}$ , this yields

$$\begin{aligned} g_{11} + g_{\emptyset} - 2g_1 &= \vec{G}_{\text{vot}} g_1 = \vec{G}_{\text{reb}} \vec{f}_1(1) = 2, \\ g_{111} + g_1 - 2g_{11} &= \vec{G}_{\text{vot}} g_{11} = \vec{G}_{\text{reb}} \vec{f}_{11}(1) = 0, \\ g_{1111} + g_{11} - 2g_{111} &= \vec{G}_{\text{vot}} g_{111} = \vec{G}_{\text{reb}} \vec{f}_{111}(1) = 0, \\ &\text{etcetera} \end{aligned} \quad (4.12)$$

Since  $\vec{f}_{\emptyset}(\alpha) = 0$  and  $\vec{f}_1(\alpha) = 1$  we have  $g_{\emptyset} = g_1 = 0$  and we can solve  $g_x$  inductively for  $x = 11, 111, 1111, \dots$  from (4.12).

The fact that the critical point and various other functions of the invariant law are different for the one-sided and two-sided model implies that the law of  $\vec{Y}_{\infty}$  cannot be mirror symmetric. Indeed, we observe that the functions  $\vec{f}_{1011}(\alpha)$  and  $\vec{f}_{1101}(\alpha)$  are not identical, as show in Figure 17.

## 4.2 Frequencies for three and more particles

As in the previous section, letting  $\overleftarrow{Y}_{\infty}$  denote the equilibrium interface process for the one-sided rebellious voter model, we have plotted in Figure 18 (picture on top left) the functions

$$\chi_k(\alpha) = \mathbb{P}[|\overleftarrow{Y}_{\infty}| = k] \quad (k = 1, 3, 5, \dots). \quad (4.13)$$

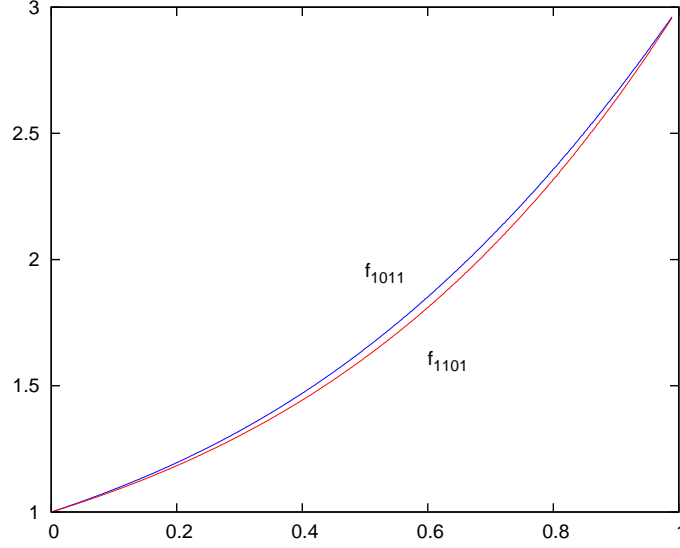


Figure 17: The functions  $\vec{f}_{1011}$  and  $\vec{f}_{1101}$  for the one-sided model, demonstrating the asymmetry of  $\vec{Y}_\infty$ . Combination of data obtained with the parameters  $N = 2^{11}$ ,  $n = 2^8$ ,  $T = 10^8$ ,  $\alpha_b = 0$ ,  $\alpha_e = 0.5$  and  $N = 2^{15}$ ,  $n = 2^8$ ,  $T = 10^9$ ,  $\alpha_b = 0.99$ ,  $\alpha_e = 0.51$ .

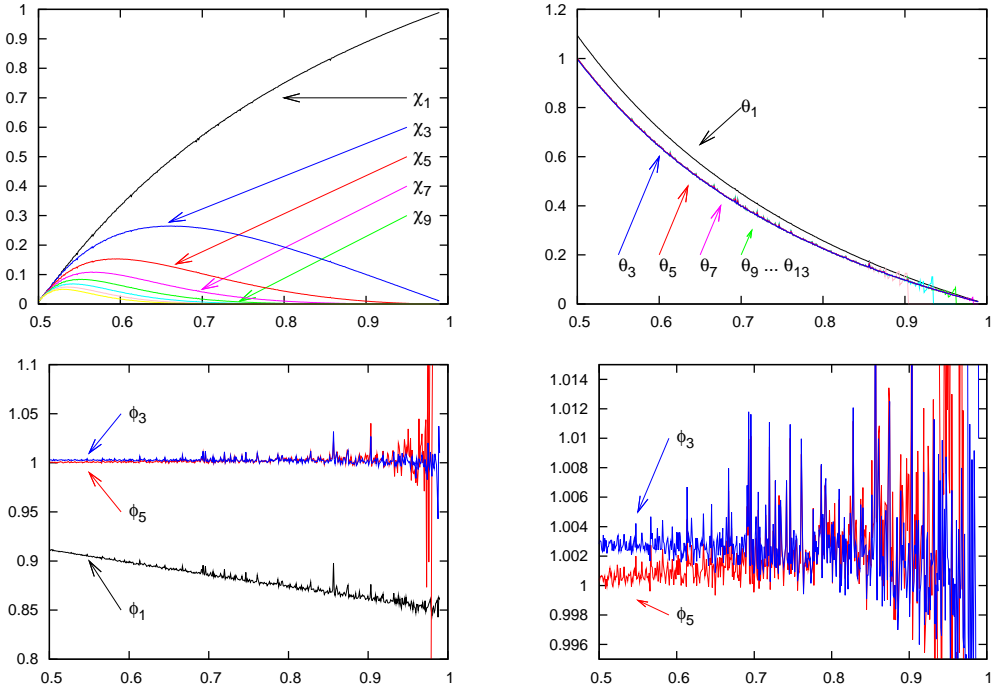


Figure 18: The frequency  $\chi_k(\alpha) = \mathbb{P}[|Y_\infty| = k]$  of seeing  $k$  particles for  $k = 1, 3, 5, \dots$  in the one-sided model. The second and third plot show the functions  $\theta_k(\alpha) := \chi_{k+2}(\alpha)/\chi_k(\alpha)$  and  $\phi_k(\alpha) := \theta_{k+2}(\alpha)/\theta_k(\alpha)$  for the first few values of  $k = 1, 3, 5, \dots$ . The fourth plot shows detail of the third plot. Data obtained with the parameters for  $\chi$  listed in (3.4)

In particular,  $\chi_1$  is the function  $\chi$  from (3.1) (ii). Except for the case  $k = 1$  (see (3.8)), we have not found any simple explicit formulas that fit these curves. Nevertheless, some regularities may be noted. In particular, if we define

$$\theta_k(\alpha) := \frac{\chi_{k+2}(\alpha)}{\chi_k(\alpha)} \quad \text{and} \quad \phi_k(\alpha) := \frac{\theta_{k+2}(\alpha)}{\theta_k(\alpha)} \quad (k = 1, 3, 5, \dots), \quad (4.14)$$

then it seems that the functions  $\theta_k$  converge very fast to a limiting function  $\theta_\infty(\alpha) := \lim_{k \rightarrow \infty} \theta_k(\alpha)$ . (See Figure 18 picture on top right; the functions  $\theta_3, \theta_5, \dots$  all seem to fall on top of each other.) Likewise, the functions  $\phi_k$  converge very fast to the function that is identically one. (See Figure 18, two bottom pictures.) It is hard to obtain sufficiently precise data, but our best data (shown here) suggest that the function  $\phi_3$  is not identically one, although it is close. This means that the functions  $\theta_3$  and  $\theta_5$  are probably not identical, even though they almost fit each other in the picture on top right. Our numerical data are well fitted by the linear/constant functions:

$$\begin{aligned} \phi_1(\alpha) &\approx c_0 + c_1(\alpha - \tfrac{1}{2}) \quad \text{with} \quad c_0 = 0.9115 \pm 0.0015 \quad \text{and} \quad c_1 = -0.13 \pm 0.01, \\ \phi_3(\alpha) &\approx 1.0027 \pm 0.0005. \end{aligned} \quad (4.15)$$

and  $\phi_k(\alpha) = 1$  for  $k \geq 5$ . We note that if one assumes that the explicit formula for  $\chi_1(\alpha)$  in (3.8) is correct, and one knows the functions  $\phi_k(\alpha)$  for each  $k = 1, 3, \dots$ , then using the fact that  $\sum_{n=0}^{\infty} \chi_{2n+1}(\alpha) = 1$  one has enough equations to solve the functions  $\chi_k(\alpha)$  for each  $k = 1, 3, \dots$ .

The limiting function  $\theta_\infty(\alpha) := \lim_{k \rightarrow \infty} \theta_k(\alpha)$  seems to be strictly decreasing and concave on  $[\frac{1}{2}, 1]$  and satisfy  $\theta_\infty(\frac{1}{2}) = 1$ ,  $\theta_\infty(1) = 0$ . This implies that the distribution of the number of particles in equilibrium has an exponentially decaying tail for each  $\alpha > \frac{1}{2}$ . In particular, the mean number of particles

$$\mu(\alpha) := \mathbb{E}[|Y_\infty|] \quad (4.16)$$

is finite for all  $\alpha > \frac{1}{2}$  and diverges as  $\alpha \downarrow \frac{1}{2}$ .

The picture for the (two-sided) rebellious voter model is extremely similar, except that the critical point is no longer 0.5 and we have no explicit formula for  $\chi_1(\alpha)$ .

### 4.3 Edge speeds

Let  $Y_t$  be the interface model of the (two- or one-sided) rebellious voter model started with a finite number of ones and let

$$l_t := \inf\{i \in \mathbb{Z} : Y_t(i) = 1\} \quad \text{and} \quad r_t := \sup\{i \in \mathbb{Z} : Y_t(i) = 1\} \quad (4.17)$$

denote the position of the left-most and right-most ones, respectively. Our simulations suggest that there exist constants  $v_-(\alpha) \leq v_+(\alpha)$ , called the *left* and *right edge speed*, respectively, such that

$$\lim_{t \rightarrow \infty} \frac{l_t}{t} = v_-(\alpha) \quad \text{and} \quad \lim_{t \rightarrow \infty} \frac{r_t}{t} = v_+(\alpha) \quad \text{a.s.} \quad (4.18)$$

Set

$$Z_t(i) := Y_t(l_t + i) \quad (i \geq 0, t \geq 0). \quad (4.19)$$

Then  $Z_t$  describes the process  $Y_t$  as seen from the left-most one. It seems reasonable to assume that the law of  $Z_t$  converges as  $t \rightarrow \infty$  to some equilibrium law. Let  $Z_\infty$  denote the process

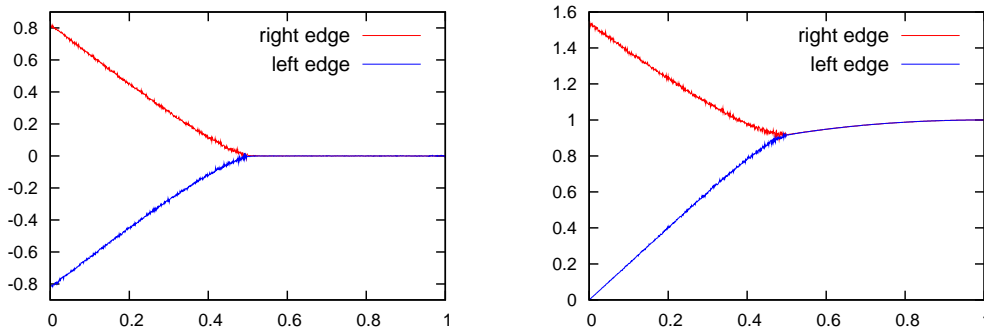


Figure 19: Edge speeds for the rebellious voter model (left) and its one-sided counterpart (right). The pictures show the speed of the right edge and left edge as a function of  $\alpha$ . Parameters used are  $N = 2^{11}$ ,  $n = 2^9$ ,  $T = 10^9$ ,  $\alpha_b = 0$ ,  $\alpha_e = 0.5$  (left half of each picture) and  $N = 2^{11}$ ,  $n = 2^9$ ,  $T = 10^{11}$ ,  $\alpha_b = 0.999$ ,  $\alpha_e = 0.5$  (right half of each picture).

in equilibrium. The left edge speed  $v_-(\alpha)$  can be obtained as the equilibrium expectation  $\mathbb{E}[f(Z_\infty)]$  of a suitable function  $f$  which sums the sizes of all possible changes of  $l_t$  multiplied with the rate at which they occur.

We have simulated the process  $Z_t$  on a finite interval of  $N$  sites by neglecting all particles that fall off the right edge of the interval due to the dynamics of  $Y_t$  or the shifts in  $l_t$ . This process does not preserve parity, but if  $N$  is large enough the probability that all particles annihilate each other is very small. For most of our data points, such events never occurred, and when they occurred (especially near the critical point) they were so rare that they likely had no big influence on our estimate of the speeds. By slowly lowering or raising  $\alpha$  in our usual fashion and keeping track of all changes in  $Z_t$  that correspond to a change in  $l_t$  we obtained numerical data for the left edge speed  $v_-(\alpha)$  and, in a similar fashion, also for the right edge speed  $v_+(\alpha)$ , both for the two-sided and one-sided model.

The results are shown in Figure 19. One has  $v_-(\alpha) < v_+(\alpha)$  if and only if  $\alpha < \alpha_c$  and the functions  $v_-(\alpha)$  and  $v_+(\alpha)$  are strictly increasing resp. decreasing on  $[0, \alpha_c]$ . For the two-sided model, by symmetry,  $v_-(\alpha) = -v_+(\alpha)$  and hence  $v_-(\alpha) = 0 = v_+(\alpha)$  for  $\alpha \geq \alpha_c$ , while for the one-sided model one has  $0 \leq v_-(\alpha)$ , but otherwise the two pictures are remarkably similar. A detailed simulation near the critical point (shown in Figure 20) shows that the estimates for the critical points which one obtains from these simulations are consistent with our earlier estimates. Apart from the obvious values  $v_-(0) = 0$  and  $v_-(1) = v_+(1) = 1$  (for the one-sided model) and  $v_- = v_+ = 0$  on  $[\alpha_c, 1]$  (for the two-sided model) we are not able to say anything explicit about the curves  $v_-(\alpha)$  and  $v_+(\alpha)$ .

## 5 Conclusions

We have simulated two one-dimensional models of parity preserving branching and annihilating random walks, which arise as the interface models of the (two-sided) rebellious voter model introduced in [SS08a] and the one-sided rebellious voter model introduced in the present paper, respectively. Both models appear to go through a phase transition between an active and an inactive phase as the parameter  $\alpha$  (which is one minus the branching rate) is increased from zero to one. In most aspects, the processes behave very similarly both qualitatively and

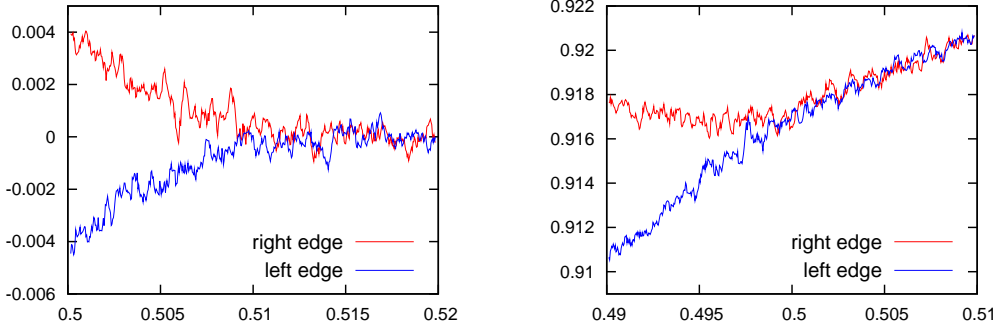


Figure 20: Detail of Figure 19. Parameters used are  $N = 2^{15}$ ,  $n = 2^9$ ,  $T = 10^{11}$ , with  $\alpha_b = 0.52$ ,  $\alpha_e = 0.5$  for the two-sided model and  $\alpha_b = 0.51$ ,  $\alpha_e = 0.49$  for the one-sided model. The curves have been smoothed, corresponding to (effectively)  $n = 2^6$ .

quantitatively.

A peculiar property of the one-sided model, however, is that both the particle density  $\rho$  and the equilibrium probability of finding a single particle  $\chi$ , defined in (2.16) and (2.18), appear to be given by explicit formulas, and the critical value appears to be exactly  $\alpha_c = \frac{1}{2}$ . We have no idea why the one-sided model, which has less symmetry than the two-sided model, should be more tractable than the latter.<sup>1</sup> In fact, most hypothetical explanations that come to one's mind should apply to the two-sided model as well, for which our numerical data convincingly show that the formulas in (3.8) do not fit. We have tried without success to find explicit formulas for other functions of our processes.

An important question is whether our proposed formulas in (3.8) for the functions  $\rho$  and  $\chi$  of the one-sided model are exact or only good approximations. In formulas (3.5) and (4.15), we have seen examples of explicit formulas containing some 'strange' constants that fit the numerical data for certain functions of the one-sided and two-sided model, respectively, within the precision of our simulations. In these examples, we believe the given formulas are probably not exact but more or less coincidentally close to the real functions. On the other hand, after trying for a considerable while to find explicit formulas for other functions of the processes, as we did, without success, one really starts to appreciate how well the simple formulas in (3.8) fit our data. The explicit formula for  $\rho$  has moreover been upheld in repeated more precise simulations near the critical point. Thus, our present position is that these formulas are probably exact, even though we have no theoretical explanation for this.

An important consequence of our proposed formula for the particle density  $\rho$  of the one-sided rebellious voter model, if it is exact, is that it implies that the order parameter critical exponent  $\beta$  for this model is one. By the principle of universality, one then expects this to be true for the whole PC universality class. It is presently generally believed that  $\beta$  is somewhat smaller than one. Recent estimates are  $\beta = 0.92(2)$  [Hin00] and  $\beta = 0.95(1)$  [OM06], although older numerical work in [IT98] yielded an estimate consistent with  $\beta = 1$ .

<sup>1</sup>Perhaps the only aspect in which the one-sided model is potentially simpler than the two-sided model is that in the former, information is passed only from left to right. A third model, which we have only studied briefly, in which voter model updates look to the right and rebellious updates look to the left, seems to have a critical point  $\alpha_c = 0.510 \pm 0.003$  and functions  $\rho, \chi$  that are close, but not identical to those of the two-sided rebellious voter model.



A thorough discussion of the reliability of these estimates lies out of the scope of the present paper. We stress that while our proposed formula for  $\rho$  strongly suggests that  $\beta = 1$ , the most convincing data for the correctness of this formula are obtained some distance away from the critical point. Our best data near the critical point are not good enough to convincingly distinguish between  $\beta = 0.92$  and  $\beta = 1$ ; see Figure 10.

It is currently believed that for the PC universality class (in dimension one),  $\beta/\nu_{\perp} = \frac{1}{2}$ . If also  $\beta = 1$ , this suggests that the static critical exponents of this universality class are simple. (The dynamical critical exponents, such as those related to the edge speeds, could still be nontrivial.) In this context, it is interesting to note the effect, observed in Section 4.1, that the harmonic function  $\vec{f}_x(\alpha)$  defined there appears to continue smoothly across the critical point, which also suggests simple critical behavior.

We conclude this paper with some suggestions for further work. First of all, the proposed formulas (3.8) ask for a theoretical explanation. This does not seem to be easy. The task would be easier if one could find explicit formulas for more functions. In particular, if one could find explicit formulas for the harmonic functions  $\vec{f}_x(\alpha)$  defined in Section 4.1, then it would be straightforward to prove that these are indeed harmonic, which probably could be used to prove (3.8) as well. For those interested in such problems, we have made the data underlying our figures available in the supplementary material. Even in the absence of an explicit formula, these harmonic functions (and their observed smooth behavior) seem a fruitful object for further theoretical considerations.

Our paper also calls for a critical evaluation of the evidence collected so far about the order parameter critical exponent  $\beta$  of the PC universality class. Finally, it raises the question if there are more models in this universality class that are (or appear to be) explicitly solvable. Our present work suggests that such models might in particular be expected in the class of one-sided models, where information is passed in one direction only.

## References

- [BEM06] J. Blath, A. Etheridge, and M. Meredith. Coexistence in locally regulated competing populations and survival of branching annihilating random walk. *Ann. Appl. Probab.* 17(5-6), 1474–1507, 2007.
- [CCDDM05] L. Canet, H. Chaté, B. Delmotte, I. Dornic, and M.A. Muñoz. Nonperturbative fixed point in a nonequilibrium phase transition. *Phys. Rev. Lett.* 95, 100601, 2005.
- [CD95] J.T. Cox and R. Durrett. Hybrid zones and voter model interfaces. *Bernoulli* 1(4): 343–370, 1995.
- [CMP09] J.T. Cox, M. Merle, and E.A. Perkins. Co-existence in a two-dimensional Lotka-Volterra model. Preprint, 2009.
- [CP06] J.T. Cox and E.A. Perkins. Survival and coexistence in stochastic spatial Lotka-Volterra models. *Probab. Theory Relat. Fields* 139(1-2), 89–142, 2007.
- [CS73] P. Clifford and A. Sudbury. A model for spatial conflict. *Biometrika* 60, 581–588, 1973.

- [CT98] J.L. Cardy and U.C. Täuber. Field theory of branching and annihilating random walks. *J. Stat. Phys.* 90, 1–56, 1998.
- [GKT84] P. Grassberger, F. Krause and T. von der Twer. A new type of kinetic critical phenomenon *J. Phys. A: Math. Gen.* 17, 105–109, 1984.
- [Gri79] D. Griffeath. *Additive and Cancellative Interacting Particle Systems*. Lecture Notes in Math. 724, Springer, Berlin, 1979.
- [Hin00] H. Hinrichsen. Nonequilibrium critical phenomena and phase transitions into absorbing states. *Adv. Phys.* 49(7), 815–958, 2000.
- [HL75] R. Holley and T.M. Liggett. Ergodic theorems for weakly interacting systems and the voter model. *Ann. Probab.* 3, 643–663, 1975.
- [IT98] N. Inui and A.Yu. Tretyakov. Critical behavior of the contact process with parity conservation. *Phys. Rev. Lett.* 80(23), 5148–5151, 1998.
- [Jen94] I. Jensen. Critical exponents for branching annihilating random walks with an even number of offspring. *Phys. Rev. E* 50(5), 3623–3633, 1994.
- [NP99] C. Neuhauser and S.W. Pacala. An explicitly spatial version of the Lotka-Volterra model with interspecific competition. *Ann. Appl. Probab.* 9(4): 1226–1259, 1999.
- [OS05] G. Ódor and A. Szolnoki. Cluster mean field study of the parity-conserving phase transition. *Phys. Rev. E* 71(6), 066128, 2005.
- [OM06] G. Ódor and N. Menyhárd. Critical behavior of an even-offspringed branching and annihilating random-walk cellular automaton with spatial disorder. *Phys. Rev. E* 73, 036130, 2006.
- [SS08a] A. Sturm and J.M. Swart. Voter models with heterozygosity selection. *Ann. Appl. Probab.* 18(1), 59–99, 2008.
- [SS08b] A. Sturm and J.M. Swart. Tightness of voter model interfaces. *Electron. Commun. Probab.* 13, paper No. 16, 165–174, 2008.
- [Sud90] A. Sudbury. The branching annihilating process: an interacting particle system. *Ann. Probab.* 18: 581–601, 1990.
- [TT92] H. Takayasu and A.Yu. Tretyakov. Extinction, survival, and dynamical phase transition of branching annihilating random walk. *Phys. Rev. Lett.* 68(20), 3060–3063, 1992.